

Turing and Hopf Bifurcation in a Diffusive Tumor-immune Model*

Jingnan Wang^{1,†} and Shengnan Liu¹

Abstract In order to understand the effect of the diffusion reaction on the interaction between tumor cells and immune cells, we establish a tumor-immune reaction diffusion model with homogeneous Neumann boundary conditions. Firstly, we investigate the existence condition and the stability condition of the coexistence equilibrium solution. Secondly, we obtain the sufficient and necessary conditions for the occurrence of Turing bifurcation and Hopf bifurcation. Thirdly, we perform some numerical simulations to illustrate the complex spatiotemporal patterns near the bifurcation curves. Finally, we explain spatiotemporal patterns in the diffusion action of tumor cells and immune cells.

Keywords Tumor-immune model, Diffusion, Hopf bifurcation, Turing bifurcation, Stability.

MSC(2010) 34C23, 35K57.

1. Introduction

The immune system of a body can monitor the development of tumor cells, and kill them by immune mechanisms [1]. However, immune responses frequently fail to prevent the growth of tumor cells. The reason is that tumor cells can escape the immune attack of the body in many ways, including low immunogenicity of tumor cells, down-regulation of MHC class I molecules, and the lack co-stimulatory molecules. Recently, a growing body of evidence supports the conclusion that a combination of immunotherapy with conventional chemotherapy and radiotherapy may improve the outcome for treating tumors. Therefore, researchers have been shifting their focus from the method of cancer treatment to the research of tumor immunotherapy mechanisms, which arouse great interest among medical scientists, biomathematicians and statisticians in [7–10, 12–15].

In 1973, Steinman discovered that dendritic cells (DC) are the most powerful antigen-presenting cells. Immature dendritic cells have strong migration ability, which can directly ingest antigens through phagocytosis and endocytosis. Mature dendritic cells present antigens to T cells, and improve the activation of B cells. In 2012, Paluka and Banichereau [12] studied the cancer immunotherapy via dendritic cell. In 2015, Nagata and Furuta et al. constructed a mathematical model representing dynamical behaviors of T cell tumor response under the support of dendritic

[†]the corresponding author.

Email address: wangjingnan@hrbust.edu.cn (J. Wang)

¹Department of Applied mathematics, Harbin University of Science and Technology, Harbin, Heilongjiang 150080, China

*The authors were partially supported by National Natural Science Foundation of China (No. 11801122) and the Natural Science Foundation of Heilongjiang Province (No. A2018008).

cells in [9]. They obtained that mutual dependence of dendritic cells and T cells in activation and tumor elimination leads to bistability between tumor immune escape and control states (immunosuppressive states). In 2016, Nakada and Nagata et al. constructed and analyzed a new mathematical model describing tumor killing by T cell response under the support of dendritic cells in [10]. In their models, there exist a handling time representing a waiting time required for T cells to be activated during antigen presentation as follows:

$$\begin{cases} \frac{dC_H(t)}{dt} = r \left(1 - \frac{C_H(t)}{K}\right) C_H(t) - cC_H(t)N_T(t) \\ \frac{dN_T(t)}{dt} = \frac{\bar{b}N_{DC}(t)}{h_{DC} + N_{DC}(t)} N_T(t) - \delta_T N_T(t) \\ \frac{dN_{DC}(t)}{dt} = aN_T(t)C_H(t) - \delta_{DC} N_{DC}(t) \end{cases} \quad (1.1)$$

where C_H, N_{DC} and N_T denote the densities of tumor, dendritic cells, and activated T cells respectively. r denotes replication rate, and K denotes carrying capacity. c denotes proportionality constant of tumor elimination by activated T cells. \bar{b} represents the T cell conversion rate under the action of dendritic cells and T cells, and a denotes the activation rate of dendritic cell by the mass action of activated T cells and tumors. δ_{DC} and δ_T denote in-activation rates of dendritic and T cells respectively. h_{DC} denotes the waiting time of T cell activation upon antigen presentation.

To investigate the mathematical property of (1.1) in more details, Nakada et al. applied the quasi-steady state approximation to system (1.1) by assuming that δ_{DC} is sufficiently large in [10], by substituting $N_{DC}(t) = \frac{aN_T(t)C_H(t)}{\delta_{DC}}$ into system (1.1), and by denoting $h = \frac{h_{DC}\delta_{DC}}{a}$, $\delta = \delta_T$, and obtained a reduced system as follows

$$\begin{cases} \frac{dC_H(t)}{dt} = r \left(1 - \frac{C_H(t)}{K}\right) C_H(t) - cC_H(t)N_T(t) \\ \frac{dN_T(t)}{dt} = \frac{\bar{b}C_H(t)N_T^2(t)}{h + C_H(t)N_T(t)} - \delta N_T(t) \end{cases} \quad (1.2)$$

In fact, some tumor cells will enter the circulating blood and invade other tissues or organs (such as chronic and acute myelogenous Leukemia [6, 20]), which arouse our interest in studying the dynamics of diffusion reaction on the interaction between tumor cells (myelogenous cells) and immune cells. In [6, 20], we know that Chronic Myelogenous Leukemia (CML) is a cancer that results in the overproduction of immature white blood cells. The main characteristic of Chronic Myelogenous Leukemia is that immature leukocytes uncontrollably proliferate in the bone marrow, and inhibit normal hematopoiesis of the bone marrow. Then, large numbers of immature leukocytes are in the circulating blood through the blood vessels, and spread throughout various tissues (and organs). Therefore, in this paper, we introduce the diffusion term into model (1.2) to describe the spread behaviors of tumor cells (myelogenous cells) and immune cells in the circulating blood. Furthermore, we study the dynamics of the diffusive tumor-immune model.

This paper is organized as follows: In Section 2, we present the existence condition and the stable condition of the coexistence equilibrium solution. In addition, we obtain sufficient and necessary conditions for the occurrence of Turing bifurcation and Hopf bifurcation. In Section 3, numerical simulations are illustrated to support analyses results and show complex spatiotemporal patterns near the bifurcation curves based on the bifurcation diagram of two parameters for the diffusive tumor-immune model. Finally, discussions and conclusions are shown in Section 4.

2. Stability and bifurcation

In this section, based on [3, 6, 11, 23], considering the spread characteristic of tumor cells (myelogenous cells) in the circulating blood through the blood vessels, we introduce the diffusion action into model (1.2), and obtain the following reaction-diffusion system describing tumor cells and immune cells under homogeneous Neumann boundary conditions.

$$\begin{cases} \frac{\partial u(x,t)}{\partial t} = d_1 \Delta u(x,t) + ru(x,t) \left(1 - \frac{u(x,t)}{K}\right) - cu(x,t)v(x,t) & x \in \Omega, t > 0 \\ \frac{\partial v(x,t)}{\partial t} = d_2 \Delta v(x,t) + \frac{\tilde{b}u(x,t)v^2(x,t)}{h+u(x,t)v(x,t)} - \delta v(x,t) & x \in \Omega, t > 0 \\ \frac{\partial u(x,t)}{\partial \nu} = 0, \frac{\partial v(x,t)}{\partial \nu} = 0 & x \in \partial\Omega, t > 0 \\ u(x,0) = u_0(x) \geq 0, v(x,0) = v_0(x) \geq 0 & x \in \bar{\Omega}, \end{cases} \tag{2.1}$$

where $u(x,t) = C_H(x,t)/C_H^0$ and $v(x,t) = N_T(t)/N_T^0$ ($C_H^0 = N_T^0 = 10^6$ as the order-of-magnitude concentration scale for tumor cells and T cells) stand for the scaled number of tumor cells (myelogenous cells) and T cells at location $x \in \Omega$ and time $t \geq 0$ respectively. Since we consider the interaction between tumor cells (myelogenous cells) and immune cells (T cells) in the one-dimensional blood vessel, we assume that the space variable is a one-dimensional space $\Omega = (0, l\pi)$ (l is a positive integer), where ν is the outward unit normal vector of the boundary $\partial\Omega$. The zero-flux boundary condition means that there are no tumor cells (myelogenous cells) or immune cells (T cells) crossing the blood vessel tissue boundary, which has been applied in many diffusion-type modelings of tumors [3, 11, 23]. d_1 denotes the diffusion coefficient of tumor cells (myelogenous cells), which is a positive constant. d_2 denotes the diffusion coefficient of immune cells (T cells), and ρ is the diffusion ratio of tumor cells (myelogenous cells) and immune cells (T cells), i.e. ($d_2 = \rho d_1$), $u_0(x)$ and $v_0(x)$ denote initial functions, which are nonnegative and continuous. r is the replication rate of tumor cells, c is the tumor killing rate by T cells, K represents the maximum capacity of tumor cells, \tilde{b} represents the tumor cell (myelogenous cell) conversion rate under the action of T cells and h represents the waiting time of T cell activation upon antigen presentation. δ is the in-activation rate of T cells.

For the sake of convenience, by applying the following scalings: $\frac{ch}{r} \rightarrow c, \frac{\tilde{b}}{\delta} \rightarrow b, \frac{v}{h} \rightarrow v, rt \rightarrow t, \frac{d_1}{r} \rightarrow d_1, \frac{d_2}{r} \rightarrow d_2$, system (2.1) is simplified as follows:

$$\begin{cases} \frac{\partial u(x,t)}{\partial t} = d_1 \Delta u(x,t) + u(x,t) \left(1 - \frac{u(x,t)}{K}\right) - cu(x,t)v(x,t) & x \in (0, l\pi), t > 0 \\ \frac{\partial v(x,t)}{\partial t} = d_2 \Delta v(x,t) + \delta v(x,t) \left(\frac{bu(x,t)v(x,t)}{1+u(x,t)v(x,t)} - 1\right) & x \in (0, l\pi), t > 0 \\ u_x(0,t) = u_x(l\pi,t) = v_x(0,t) = v_x(l\pi,t) = 0, t > 0 \\ u(x,0) = u_0(x) \geq 0, v(x,0) = v_0(x) \geq 0 & x \in [0, l\pi]. \end{cases} \tag{2.2}$$

Obviously, both $E_0 = (0,0)$ and $E_K = (K,0)$ are always constant equilibrium solutions of system (2.2). Referring to the stability result of equilibrium solutions in [10], we know that the equilibrium solution E_K is stable. If there exists a positive constant equilibrium solution (u^*, v^*) of (2.2), then u^* and v^* satisfy the following algebraic equations:

$$u^{*2} - Ku^* + \frac{cK}{b-1} = 0, v^* = \frac{K-u^*}{Kc} \tag{2.3}$$

Since $\tilde{b} > \delta$ in system (2.1), $b > 1$ in system (2.2). By combining algebraic equation (2.3), we obtain the existence condition of the positive constant equilibriums of system (2.2).

Lemma 2.1. *The existence of positive constant steady states of system (2.2) is as follows:*

- i) If $c < \frac{K(b-1)}{4}$, then system (2.2) has two positive constant steady states $E_{\pm}^* = (u_{\pm}^*, v_{\pm}^*)$, where

$$u_{\pm}^* = \frac{K \pm \sqrt{K^2 - \frac{4Kc}{b-1}}}{2}, \quad v_{\pm}^* = \frac{K - u_{\pm}^*}{Kc}. \quad (2.4)$$

- ii) If $c = \frac{K(b-1)}{4}$, then system (2.2) has a unique positive constant steady state $E^* = (u^*, v^*)$, where $u^* = \frac{K}{2}$, $v^* = \frac{K-u^*}{Kc}$.

For the sake of convenience, we list the basic results of the stability for system (2.2) with $d_1 = 0$ and $d_2 = 0$. Throughout this paper, let

$$\delta_0 = \frac{bu_-^*}{K(b-1)}, \quad (2.5)$$

and we assume

$$(H_0) : c > \frac{(b-1)(u_-^*)^2}{K}, \quad (H_1) : c < \frac{(b-1)(u_-^*)^2}{K}.$$

Lemma 2.2. *Assume that $c < K(b-1)/4$, δ_0 is defined by (2.5).*

- i) If $c < \frac{(b-1)(u_+^*)^2}{K}$, then the positive constant steady state E_+^* is unstable for system (2.2) with $d_1 = 0$ and $d_2 = 0$;
- ii) If $\delta < \delta_0$ and condition (H_0) holds, then the positive constant steady state E_-^* is locally asymptotically stable for system (2.2) with $d_1 = 0$ and $d_2 = 0$;
- iii) If $\delta < \delta_0$ and condition (H_1) holds, then the positive constant steady state E_-^* is a saddle point for system (2.2) with $d_1 = 0$ and $d_2 = 0$;
- iv) If $\delta > \delta_0$ and condition (H_0) holds, then the positive constant steady state E_-^* is unstable for system (2.2) with $d_1 = 0$ and $d_2 = 0$.

Next, we study effects of the diffusion factor on the positive constant steady state E_-^* of system (2.2) based on the bifurcation analyses such as Turing bifurcations and Hopf bifurcations.

Linearizing system (2.2) at E_-^* , we have

$$\begin{cases} \frac{\partial u(x,t)}{\partial t} = d_1 \Delta u - \frac{u_-^*}{K} (u - u_-^*) - cu_-^* (v - v_-^*) \\ \frac{\partial v(x,t)}{\partial t} = d_2 \Delta v + \frac{\delta}{b(u_-^*)^2} (u - u_-^*) + \delta \left(1 - \frac{1}{b}\right) (v - v_-^*). \end{cases} \quad (2.6)$$

Then, system (2.6) can be written as an abstract differential equation in the phase space X of the form

$$\begin{pmatrix} u_t \\ v_t \end{pmatrix} = L \begin{pmatrix} u \\ v \end{pmatrix} \triangleq \mathcal{D} \begin{pmatrix} u_{xx} \\ v_{xx} \end{pmatrix} + J \begin{pmatrix} u \\ v \end{pmatrix} \quad (2.7)$$

where

$$X \triangleq \left\{ (u, v) \in H^2(0, l\pi) \times H^2(0, l\pi) \mid \frac{\partial u}{\partial x} \Big|_{x=0, l\pi} = \frac{\partial v}{\partial x} \Big|_{x=0, l\pi} = 0 \right\}.$$

$H^2(0, l\pi)$ denotes the standard Sobolev space, and

$$\mathcal{D} = \begin{pmatrix} d_1 & 0 \\ 0 & d_2 \end{pmatrix}, J = \begin{pmatrix} \frac{-u_-^*}{K} & -cu_-^* \\ \frac{\delta}{b(u_-^*)^2} & \delta \left(1 - \frac{1}{b}\right) \end{pmatrix}.$$

Thus, the characteristic equations of system (2.7) are

$$F_k(\lambda) = \lambda^2 + T_k(d_1, d_2)\lambda + D_k(d_1, d_2) = 0, \tag{2.8}$$

where

$$T_k(d_1, d_2) = \frac{u_-^*}{K} - \delta \left(1 - \frac{1}{b}\right) + (d_1 + d_2) \frac{k^2}{l^2}, \tag{2.9}$$

$$D_k(d_1, d_2) = d_1 d_2 \frac{k^4}{l^4} + \left(\frac{d_2 u_-^*}{K} - \delta d_1 \left(1 - \frac{1}{b}\right) \right) \frac{k^2}{l^2} + \frac{\delta c}{b u_-^*} - \delta \left(1 - \frac{1}{b}\right) \frac{u_-^*}{K} \tag{2.10}$$

with $k = 0, 1, 2, \dots$.

Based on the research methods in [2, 4, 5, 16–19, 22], we discuss the existence conditions of Turing bifurcation and Hopf bifurcation points under the condition $c < K(b - 1)/4$. According to paper [5], we know that all the eigenvalues of (2.8) with $k = 0$ have negative real parts. In the remaining parts, k -mode Turing (Hopf) bifurcation is referred to as the corresponding k -th characteristic equation having a zero root (a pair of purely imaginary roots). Moreover, since the transversality conditions hold, Turing bifurcation and Hopf bifurcation occur respectively [5]. If k is a positive integer, then k -mode Hopf bifurcation is also called wave bifurcation [17, 19].

2.1. Turing bifurcation and Turing instability

Theorem 2.1. Assume that $\frac{(b-1)(u_-^*)^2}{K} < c < K(b - 1)/4$. Let

$$\delta_k(d_1) = \frac{b u_-^* (d_1 d_2 \frac{k^4}{l^4} + d_2 \frac{k^2}{l^2} \frac{u_-^*}{K})}{(b - 1) \left(d_1 \frac{k^2}{l^2} + \frac{u_-^*}{K} \right) u_-^* - c}. \tag{2.11}$$

If $d_1 > d_2$ and $\delta < \frac{b u_-^*}{K(b-1)}$ hold, then system (2.2) undergoes Turing bifurcation at $\delta = \delta_k(d_1)$, when there exists a positive integer k satisfying $d_1 > \frac{Kc - (b-1)(u_-^*)^2}{K(b-1) \frac{k^2}{l^2} u_-^*}$.

Proof. Using the same methods of papers [17, 19], from (2.10), we obtain that if $\frac{(b-1)(u_-^*)^2}{K} < c$ and $\delta < \frac{u_-^*}{K(b-1)}$, then $T_0(0, 0) > 0$ in (2.9) and $D_0(0, 0) > 0$ in (2.10). That is to say, all the roots of (2.8) for $k = 0$ have strictly negative real parts. Thus, the constant steady state E_-^* of system (2.2) with $d_1 = 0$ and $d_2 = 0$ is stable. By computing, we know that if $d_1 > d_2$, then $D_k(d_1, d_2) = 0$ at $\delta = \delta_k(d_1)$, where k is a positive integer satisfying $d_1 > \frac{Kc - (b-1)(u_-^*)^2}{K(b-1) \frac{k^2}{l^2} u_-^*}$ as $Kc > (b - 1)(u_-^*)^2$.

That is to say, the characteristic equation (2.8) has a zero root $\lambda = 0$. Taking the derivative of both sides of equation (2.8) with respect to λ , if $\delta_k(d_1) < \delta_0$, then we have

$$\frac{dF_k(\lambda)}{d\lambda} \Big|_{\lambda=0}^{\delta=\delta_k(d_1)} = T_k(d_1, d_2) \Big|_{\delta=\delta_k(d_1)} > 0.$$

It implies that $\lambda = 0$ is a single root of equation (2.8). Furthermore, if $d_1 > \frac{Kc-(b-1)(u_*^*)^2}{K(b-1)\frac{k^2}{l^2}u_*^*}$ and $\delta_k(d_1) < \delta_0$, then we obtain

$$\frac{d(\lambda(\delta))}{d\delta} \Big|_{\lambda=0}^{\delta=\delta_k(d_1)} = \frac{(1 - \frac{1}{b}) \left(d_1 \frac{k^2}{l^2} + \frac{u_*^*}{K} \right) - \frac{c}{bu_*^*}}{T_k(d_1, d_2) \Big|_{\delta=\delta_k(d_1)}} > 0$$

where $T_k(d_1, d_2)$ is defined by (2.9), the transversality condition holds. Thus, system (2.2) satisfies the following conditions of occurring Turing bifurcation:

$$\text{Im}(\lambda_k) = 0, \text{Re}(\lambda_k) = 0, \text{ at } k \neq 0,$$

where k is a positive integer. Thus, system (2.2) undergoes turing bifurcation at $\delta = \delta_k(d_1)$ (defined by (2.11)), which is denoted as the turing bifurcation curve L_1 . This completes the proof.

In order to determine the value k for the k -model Turing bifurcation, we use the methods in [5] to determine the feasible region on the plane of diffusion ratio ρ ($\rho = d_2/d_1$) and diffusion coefficient d_1 of tumor cells, on which a Turing bifurcation curve may exist. For the sake of investigation, we choose $l = 1$ in $\Omega = (0, l\pi)$, and denote $d_1, d_2, T_k(d_1, d_2)$ and $D_k(d_1, d_2)$ as $d, \rho d, T_d(k, \rho)$ and $D_d(k, \rho)$ respectively. Thus, (2.8), (2.9) and (2.10) become

$$F_k(\lambda) = \lambda^2 + T_d(k, \rho)\lambda + D_d(k, \rho) = 0 \tag{2.12}$$

$$T_d(k, \rho) = A - D + d(1 + \rho)k^2 \tag{2.13}$$

$$D_d(k, \rho) = \rho d^2 k^4 + k^2 d(\rho A - D) + BC - AD \tag{2.14}$$

where $A = u_*^*/K, B = \frac{\delta}{b(u_*^*)^2}, C = cu_*^*, D = \delta(1 - \frac{1}{b}), k = 0, 1, 2, \dots$.

Lemma 2.3. *For model (2.2), the Turing bifurcation point (ρ, d) always exists, and $(\rho, d) \in \{(\rho, d) \in \mathbb{R}_2^+, d > 0, 0 < \rho < \rho_B(d)\} \doteq U$, where*

$$\rho_B(d) = \begin{cases} \rho_1, & 0 < d \leq \tilde{d} \\ \rho_2(d), & d \geq \tilde{d} \end{cases} \tag{2.15}$$

where $\tilde{d} = D - \frac{AD^2}{(\sqrt{BC} - \sqrt{BC-AD})^2}, \rho_1 = \frac{(\sqrt{BC} - \sqrt{BC-AD})^2}{A^2}$ and $\rho_2(d) = \frac{D}{A+d}$.

Proof. For $k \in \mathbb{R}^+, D_d(k, \rho)$ attains its minimum when $k_{min}^2 = \frac{D-\rho A}{2\rho d}$. It can then be verified that $\min_{k \in \mathbb{R}^+} D_d(k, \rho) = (BC - AD) - \frac{(\rho A - D)^2}{4\rho} > 0$ if and only if $\rho > \rho_1$. From (H₀), we have $T_d(k, \rho) > 0$ for any $k \in \mathbb{R}^+$. Therefore, $\lambda = 0$ cannot be a root of (2.12) for any $k \in \mathbb{R}^+$ whenever $\rho > \rho_1$. In addition, if $\rho < \rho_2(d)$, then $k_{min}^2 = \frac{D-\rho A}{2\rho d} > \frac{1}{2}$. Consequently, there exists apair (ρ, d) for some $k \in \mathbb{R}^+$, such that $\rho < \rho_1$ and $\rho < \rho_2(d)$ and that $\lambda = 0$ is a root of (2.12). Since $\rho_2(d)$ is strictly

decreasing with respect to d , there exists $d = d_0 = \frac{A^2 D}{(\sqrt{BC} - \sqrt{BC - AD})^2} - A$ such that $\rho_1 = \rho_2(d_0)$, $\rho_1 < \rho_2(d)$ for $d \in (0, d_0)$ and $\rho_2(d) < \rho_1$ for $d \in (d_0, \infty)$. From the above discussion, we conclude that the Turing bifurcation point $(\rho, d) \in U$. This completes the proof.

If the characteristic equation (2.12) has a zero characteristic root for $k \in \mathbb{N}$, then there exists a positive integer $k \neq 0$ such that $D_d(k, \rho) = 0$. Thus, the value of ρ can be calculated from equation (2.14), denoted by $\rho_*(d, k)$

$$\rho_*(d, k) = D \frac{dk^2 - Z_1}{dk^2(dk^2 + A)} \tag{2.16}$$

for $d > \tilde{d}_k = \frac{BC - AD}{Dk^2}$ where $Z_1 = \frac{BC - AD}{D}$. Obviously, $D_d(k, \rho) = 0$, whenever $\rho = \rho_*(d, k)$. Using a geometric argument and the results of [5], we obtain the following properties for $\rho_*(d, k)$.

Lemma 2.4. *Suppose that $c < K(b - 1)/4$ holds. If $A - D > 0$ and $BC - AD > 0$ hold, we have the following properties for $\rho_*(d, k)$.*

- i) *For any fixed $k \in \mathbb{N}$, $\rho = \rho_*(d, k)$ reaches its maximum $\rho_1 = \frac{(\sqrt{BC} - \sqrt{BC - AD})^2}{A^2}$ at $d = d_M(k) \doteq \frac{(Z_1 + \sqrt{Z_1^2 + Z_1 A})}{k^2} > \tilde{d}_k$, and $\rho_*(d, k)$ is monotonically decreasing (increasing) with respect to d , for $d > d_M(k)$ ($\tilde{d}_k < d < d_M(k)$).*

- ii) *For any $k \in \mathbb{N}$, the equation*

$$\rho_*(d, k) = \rho_*(d, k + 1), d > 0$$

has a unique positive root $d_{k,k+1} \in (d_M(k + 1), d_M(k))$ for d , which is given by

$$d_{k,k+1} = \frac{Z_1}{2} \left[\frac{1}{k^2} + \frac{1}{(k + 1)^2} + \sqrt{\left(\frac{1}{k^2} + \frac{1}{(k + 1)^2} \right)^2 + \frac{4A}{Z_1 k^2 (k + 1)^2}} \right]. \tag{2.17}$$

Moreover,

$$\rho_*(d, k) > \rho_*(d, k + 1) > \rho_*(d, k + 2) > \dots \text{ for } d > d_{k,k+1}. \tag{2.18}$$

- iii) *Let*

$$\rho_*(d) = \rho_*(d, k) \text{ for } d \in [d_{k,k+1}, d_{k-1,k}), k \in \mathbb{N}, \tag{2.19}$$

where $d_{0,1} \doteq \infty$. Then $\rho_(d) \leq \rho_B(d)$ for $0 < d < \infty$, $\rho_*(d) = \rho_B(d)$ if and only if $d = d_M(k)$, $k \in \mathbb{N}$.*

Lemma 2.5. *Assume that $\frac{(b-1)(u^+)^2}{K} < c < K(b - 1)/4$ holds. If $A - D > 0$ and $BC - AD > 0$ hold, then we have*

- i) *If $d \in [d_{k_T, k_T+1}, d_{k_T-1, k_T})$ for some positive integer $k_T \in \mathbb{N}$ and $\rho = \rho_*(d)$, then 0 is a simple root of (2.12) with $k = k_T$, and all the other roots of (2.12) have strictly negative real parts. Furthermore, let $\lambda = \lambda(\rho, k_T)$ be*

the root of (2.12) when $k = k_T$ such that $\lambda(\rho, k_T)|_{\rho=\rho_*(d)} = 0$, where $\rho \in (\rho_*(d) - \varepsilon, \rho_*(d) + \varepsilon)$ for a sufficiently small ε . Then,

$$\left. \frac{d\lambda(k_T, \rho)}{d\rho} \right|_{\substack{\rho=\rho_*(d) \\ \lambda=0}} < 0. \quad (2.20)$$

ii) If $d = d_{k_T, k_{T+1}}$ and $\rho = \rho_*(d_{k, k+1})$, then 0 is a simple root of (2.12) for both k and $k + 1$, $k \in \mathbb{N}$.

Proof. (i) Recall that $D_d(\rho, k) = 0$, if and only if $\rho = \rho_*(d)$ for $k_T \in \mathbb{N}$. Then, for any $k \in \mathbb{N}$, $\lambda = 0$ is always a root of (2.12) with such values of k when $\rho = \rho_*(k, d)$. By the definition of $\rho_*(d)$ and $\rho_*(k, d)$, we know that for $d \in [d_{k_T, k_{T+1}}, d_{k_{T-1}, k_T})$ for some k_T and $\rho = \rho_*(d)$, then $\lambda = 0$ is a root of the characteristic equation (2.12) with $k = k_T$. Furthermore, $\lambda = 0$ is simple, since

$$\left. \frac{dF_{k_T}(\lambda, \rho)}{d\lambda} \right|_{\substack{\rho=\rho_*(d) \\ \lambda=0}} = T_d(k_T, \rho_*(d)) > 0,$$

where $T_d(k, \rho)$ is defined by (2.13). Differentiating (2.12) with respect to ρ gives

$$\left. \frac{dF_{k_T}(\lambda, \rho)}{d\rho} \right|_{\substack{\rho=\rho_*(d) \\ \lambda=0}} = T_d(k_T, \rho_*(d)) \left. \frac{d\lambda(\rho, k_T)}{d\rho} \right|_{\rho=\rho_*(d)} + d^2 k_T^4 + \frac{dk_T^2 u_*^*}{K} = 0. \quad (2.21)$$

Thus, from (2.21), we have

$$\left. \frac{d\lambda(k_T, \rho)}{d\rho} \right|_{\substack{\rho=\rho_*(d) \\ \lambda=0}} = -\frac{d^2 k_T^4 + \frac{dk_T^2 u_*^*}{K}}{T_d(k_T, \rho_*(d))} < 0,$$

where $T_d(k, \rho)$ is defined by (2.13). This proves the first statement.

(ii) By a similar argument as above, one can show the second assertion. This completes the proof.

Theorem 2.2. Assume that $\frac{(b-1)(u_*^*)^2}{K} < c < K(b-1)/4$ holds. Then, we have

- i) The condition for the occurrence of Turing instability at the positive steady state $E_-^*(u_*^*, v_*^*)$ of system (2.2) is $0 < \rho < \rho_*(d_1)$, $d_1 > 0$;
- ii) When $\rho = \rho_*(d_1)$ holds for $d \in [d_{k_T, k_{T+1}}, d_{k_{T-1}, k_T})$, system (2.2) will undergo Turing bifurcation whose wave number is k_T , where $\rho = d_2/d_1$ and $\rho_*(\cdot)$ is as defined in formula (2.19)

2.2. Hopf bifurcation and periodic solutions

Theorem 2.3. Assume that $\frac{(b-1)(u_*^*)^2}{K} < c < K(b-1)/4$. Let

$$\delta_* = \frac{bu_*^* + bK\frac{k^2}{l^2}(d_1 + d_2)}{(b-1)K}. \quad (2.22)$$

Then, we have the following results:

- i) If $\delta = \delta_0$ holds, then system (2.2) undergoes 0-mode Hopf bifurcation;

ii) If $(\frac{u_-^*}{K} + d_1 \frac{k^2}{l^2})(b-1)(u_-^* - 1) < c < (\frac{u_-^*}{K} + d_1 \frac{k^2}{l^2})(b-1)u_-^*$, $k \in (k_1, k_2)$ or $c > (\frac{u_-^*}{K} + d_1 \frac{k^2}{l^2})(b-1)u_-^*$ holds, then the characteristic equation (2.8) has a pair of simple pure imaginary roots at $\delta = \delta_*$. Additionally, system (2.2) undergoes Hopf bifurcation ($k \neq 0$), and has a periodic solution, where

$$k_{1,2} = l \sqrt{\frac{-(b-1)2d_1(u_-^*)^2 + Kc(d_1 + d_2) + \sqrt{\Theta}}{2(b-1)K(u_-^*)d_1^2}}, \tag{2.23}$$

where

$$\Theta = ((b-1)2d_1(u_-^*)^2 - Kc(d_1 + d_2))^2 - 4(b-1)(u_-^*)^2d_1^2((b-1)(u_-^*)^2 - cK).$$

Proof. Using the same methods of paper [2, 4, 17], we obtain that

i) The conditions for 0-mode Hopf bifurcation to occur are as follows:

$$\text{Im}(\lambda_k) \neq 0, \text{Re}(\lambda_k) = 0, \text{ at } k = 0.$$

If $k = 0$, then characteristic equation (2.8) becomes

$$F_0 = \lambda^2 + \left(\frac{u_-^*}{K} - \delta\left(1 - \frac{1}{b}\right)\right)\lambda + \frac{\delta c}{bu_-^*} - \delta\left(1 - \frac{1}{b}\right)\frac{u_-^*}{K} = 0. \tag{2.24}$$

Clearly, if $\frac{(b-1)(u_-^*)^2}{K} < c$ and $\delta = \frac{bu_-^*}{K(b-1)}$, that is $\delta = \delta_0$, then characteristic equation (2.8) has a pair of simple pure imaginary roots $\lambda = \pm i\omega_0$, where $\omega_0 = \sqrt{\frac{\delta_0 c}{bu_-^*} - \delta_0\left(1 - \frac{1}{b}\right)\frac{u_-^*}{K}}$. Furthermore,

$$\left.\frac{d\text{Re}(\lambda(\delta))}{d\delta}\right|_{\substack{\delta=\delta_0 \\ \lambda=i\omega_0}} = \frac{(1-1/b)}{2} > 0$$

the transversality condition holds. Thus, system (2.2) undergoes 0-mode Hopf bifurcation at $\delta = \delta_0$, denoted as the 0-mode Hopf bifurcation curve L_2 .

ii) When $k \neq 0$, we suppose that characteristic equation (2.8) has a pair of pure imaginary root, let $\lambda_k = i\omega_k$. Substituting $\lambda_k = i\omega_k$ into characteristic equation (2.8) and separating the real and imaginary parts, we have

$$\begin{cases} \frac{u_-^*}{K} + (d_1 + d_2)\frac{k^2}{l^2} - \delta\left(1 - \frac{1}{b}\right) = 0 \\ d_1d_2\frac{k^4}{l^4} + \left(d_2\frac{u_-^*}{K} - \delta\left(1 - \frac{1}{b}\right)d_1\right)\frac{k^2}{l^2} + \frac{c\delta}{bu_-^*} - \delta\left(1 - \frac{1}{b}\right)\frac{ru_-^*}{K} = \omega_k^2. \end{cases} \tag{2.25}$$

From the first equation of (2.25), we have

$$\delta = \frac{bu_-^* + bK\frac{k^2}{l^2}(d_1 + d_2)}{(b-1)K}. \tag{2.26}$$

That is, $\delta = \delta_*$. From the second equation of (2.25), we know that, if $\omega_k^2 > 0$, then

$$D_k(d_1, d_2) = d_1d_2\frac{k^4}{l^4} + \frac{k^2}{l^2}\left(\frac{d_2u_-^*}{K} - d_1\delta\left(1 - \frac{1}{b}\right)\right) + \frac{\delta c}{bu_-^*} - \delta\left(1 - \frac{1}{b}\right)\frac{u_-^*}{K} > 0. \tag{2.27}$$

Note that, by solving inequality (2.27), there are two possible cases for $\omega_k^2 > 0$.

Case (I): if $c < (\frac{u_*^*}{K} + d_1 \frac{k^2}{l^2})(b-1)u_*^*$, then from (2.27), we have

$$\delta < \frac{bu_*^*(d_1 \frac{k^4}{l^4} + \frac{k^2 u_*^*}{l^2 K})d_2}{(b-1)(d_1 \frac{k^2}{l^2} + \frac{u_*^*}{K})u_*^* - c} \doteq \tilde{\delta}. \quad (2.28)$$

By combining (2.26) and (2.28) yields $\delta_* < \tilde{\delta}$, i.e.

$$\frac{bu_*^* + bK \frac{k^2}{l^2}(d_1 + d_2)}{(b-1)K} < \frac{bu_*^*(d_1 \frac{k^4}{l^4} + \frac{k^2 u_*^*}{l^2 K})d_2}{(b-1)(d_1 \frac{k^2}{l^2} + \frac{u_*^*}{K})(u_*^*) - c}. \quad (2.29)$$

In order to find a positive integer k satisfying inequality (2.29), let $\varphi(k^2)$ be the following quadratic equation of k^2 :

$$\begin{aligned} \varphi(k^2) = & ((b-1)Kd_1^2 u_*^*) \left(\frac{k^2}{l^2} \right)^2 + ((b-1)2d_1(u_*^*)^2 - Kc(d_1 + d_2)) \frac{k^2}{l^2} \\ & + \left(\frac{(b-1)(u_*^*)^3}{K} - u_*^*c \right). \end{aligned} \quad (2.30)$$

By computing, we obtain the two solutions k_1, k_2 of $\varphi(k^2) = 0$ is defined by (2.23). By combining (2.26), (2.28) and (2.30), if $(\frac{u_*^*}{K} + d_1 \frac{k^2}{l^2})(b-1)(u_*^* - 1) < c < (\frac{u_*^*}{K} + d_1 \frac{k^2}{l^2})(b-1)u_*^*$, then $d_2 > 0$ and there exists a $k \in (k_1, k_2)$ satisfying $\varphi(k^2) < 0$. That is, inequality (2.29) holds.

Cases (II): If $c > (\frac{u_*^*}{K} + d_1 \frac{k^2}{l^2})(b-1)u_*^*$, then inequality (2.29) holds for every positive integer k .

Under the conditions of Case (I) and Case (II), if $\delta = \delta_*$, then characteristic equation (2.8) has a pair of pure imaginary root $\lambda = \pm i\omega_k$, where $\omega_k = \sqrt{D_k(d_1, d_2)}|_{\delta=\delta_*}$, $D_k(d_1, d_2)$ is defined by (2.10). Furthermore,

$$\left. \frac{d\operatorname{Re}(\lambda(\delta))}{d\delta} \right|_{\substack{\delta=\delta_* \\ \lambda=i\omega_k}} = \frac{b-1}{2b} > 0,$$

then the transversality condition holds. Therefore, whenever $(\frac{u_*^*}{K} + d_1 \frac{k^2}{l^2})(b-1)(u_*^* - 1) < c < (\frac{u_*^*}{K} + d_1 \frac{k^2}{l^2})(b-1)u_*^*$, $k \in (k_1, k_2)$ or $c > (\frac{u_*^*}{K} + d_1 \frac{k^2}{l^2})(b-1)u_*^*$, system (2.2) undergoes Hopf bifurcation ($k \neq 0$), and has a periodic solution at $\delta = \delta_*$ (see (2.22)) denoted as curve L_3 .

3. Simulations and discussion

In this section, based on our results of linear stability analysis and bifurcation analysis in Section 2 and Section 3, we perform some numerical simulations concerning system (2.2) to show the influence of the diffusion factor and the in-activation rate of T cells on the stability and spatiotemporal patterns of system (2.2) with some fixed parameters.

We choose

$$K = 20, c = 16, b = 5 \quad (3.1)$$

for system (2.2). Then, we obtain the following constant equilibrium solutions

$$E_0 = (0, 0), E_K = (20, 0), E_-^* = (5.5278, 0.04522), E_+^* = (14.4721, 0.01727).$$

By computing, we obtain that $\delta_0 = 0.3454915$. From Lemma 2.2 and Theorem 2.3, if we choose $(d_1, d_2) = (0, 0)$ and $\delta = 0.2 (< \delta_0)$ of system (2.2) with the condition (3.1), then there exists a stable steady state solution for system (2.2) without the diffusive influence (see Figure 1). If we choose $(d_1, d_2) = (0, 0)$ and $\delta = 0.3455$ of system (2.2) with the condition (3.1), then there exists a homogeneous periodic solution for system (2.2) without the diffusive influence (see Figure 2).

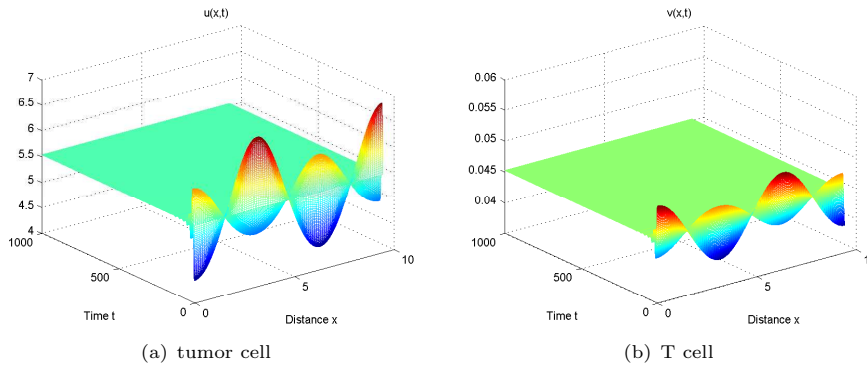


Figure 1. The stable steady state (E_-^*) of (2.2) as $t \rightarrow \infty$ for $\delta = 0.2$ and $(d_1, d_2) = (0, 0)$.

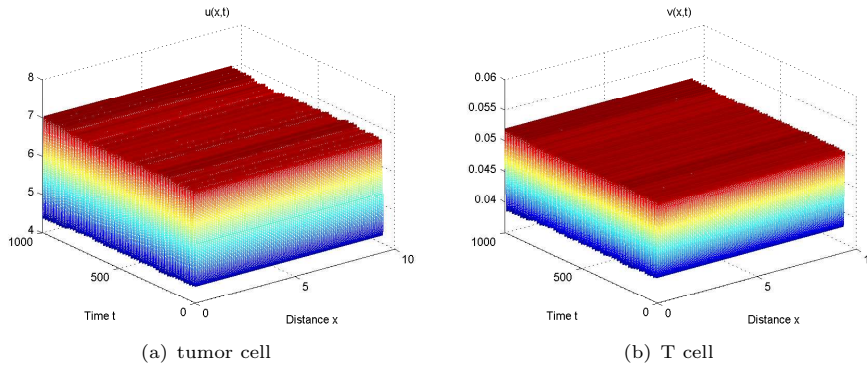


Figure 2. A homogeneous periodic solution of (2.2) for $\delta = 0.3455$ and $(d_1, d_2) = (0, 0)$

In order to show the effects of diffusion factors on tumor-immune system (2.2) in Theorem 2.1 and Theorem 2.3, we choose parameter condition (3.1) and $d_2 = 0.012675$ to determine the bifurcation curves $L_1 - L_3$ as follows:
 Turing bifurcation curve $L_1 : \delta = \delta_k(d_1) = \frac{0.3503d_1 + 0.096819}{22.11d_1 - 9.886}, d_1 > 0.4471359, \frac{k}{l} = 1$;
 Hopf bifurcation line $L_2 : \delta = \delta_0 = 0.3454915, (d_1, d_2) = (0, 0), k = 0$;
 Hopf bifurcation line $L_3 : \delta = \delta_* = 0.36133 + 1.25d_1, \frac{k}{l} = 1$.
 Then, the $d_1 - \delta$ plane is divided into seven regions I-VII (see Figure 1) by the bifurcation curves $L_1 - L_3$.

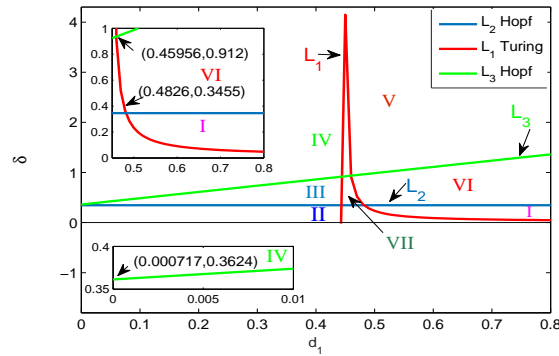


Figure 3. Bifurcation diagram $d_1 - \delta$ for system (2.2)

From Figure 3, the Turing bifurcation curve and the Hopf bifurcation lines ($k \geq 0$) intersect at codimension-2 bifurcation points. The bifurcation curves separate the parametric space into several distinct domains. Domain I is a pure Turing instability region. In domain II, located below all three bifurcation lines, the steady state E^* is the stable solution of system (2.2). Domain III is the region of Hopf instability, and domain IV is the region of periodic solution. Domain V is located above all the bifurcation curves, in which the steady state E_K is the stable solution of system (2.2). Domains VI and VII are the regions of inhomogeneous periodic solutions induced by Turing and Hopf bifurcations.

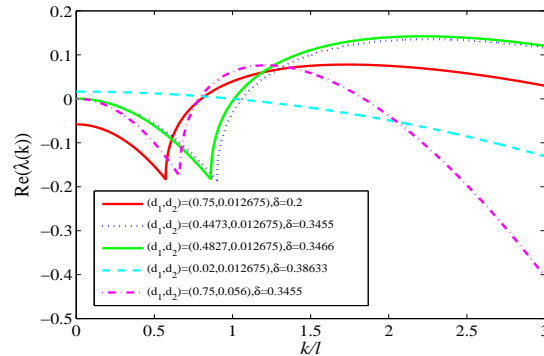


Figure 4. The Graph of $\text{Re}(\lambda(k))$ with respect to k/l with fixed $d_2 = 0.012675$

According to Figure 3, we choose the parameter condition (3.1), $d_2 = 0.012675, 0.056$, and several groups of perturbation parameter values- $(d_1, \delta) = (0.75, 0.2), (0.75, 0.3455), (0.4473, 0.3455), (0.4827, 0.3466), (0.02, 0.38633)$ to show the value of $\text{Re}(\lambda(k))$ (see Figure 2), which reveals the value of k/l when Turing instability occurs.

According to the seven regions in Figure 3 and Figure 4, we choose $d_2 = 0.012675$, parameter condition (3.1) and four groups of perturbation parameter values- $(d_1, \delta) = (0.75, 0.2), (0.02, 0.38633), (0.4827, 0.3466), (0.4473, 0.3455)$ to show the results of numerical simulations for system (2.2) as follows:

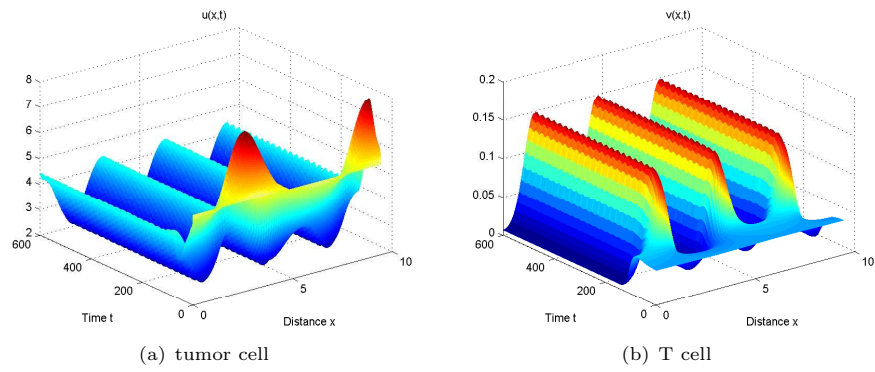


Figure 5. A spatially inhomogeneous steady state of (2.2), for $(d_1, \delta) = (0.75, 0.2) \in I$

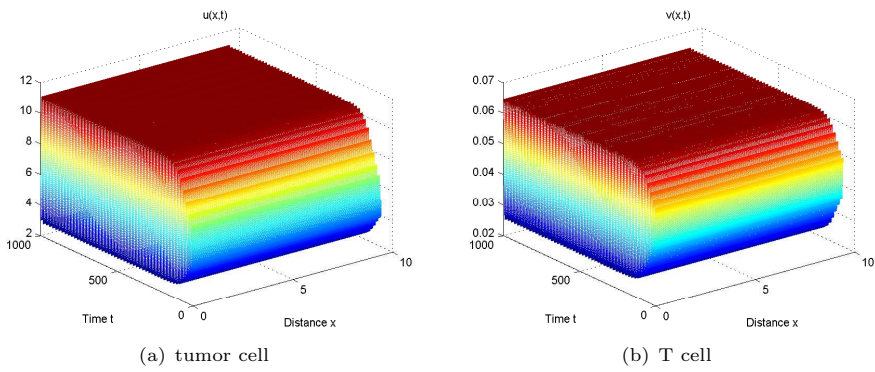


Figure 6. A homogeneous periodic solution of (2.2), for $(d_1, \delta) = (0.02, 0.38633) \in IV$

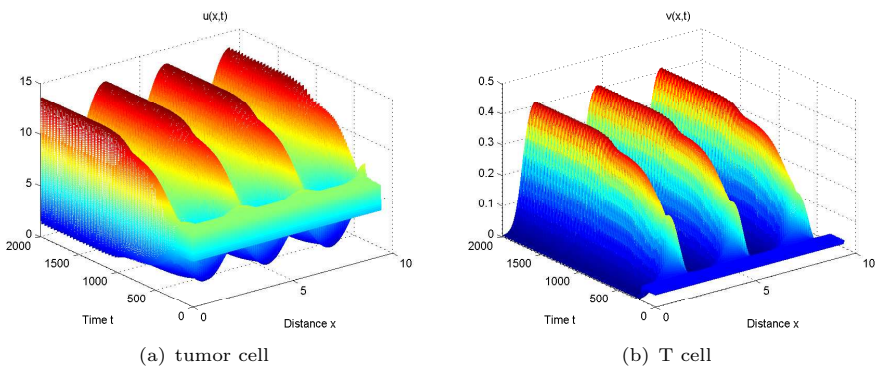


Figure 7. A spatially inhomogeneous periodic solution of (2.2), for $(d_1, \delta) = (0.4827, 0.3466) \in VI$

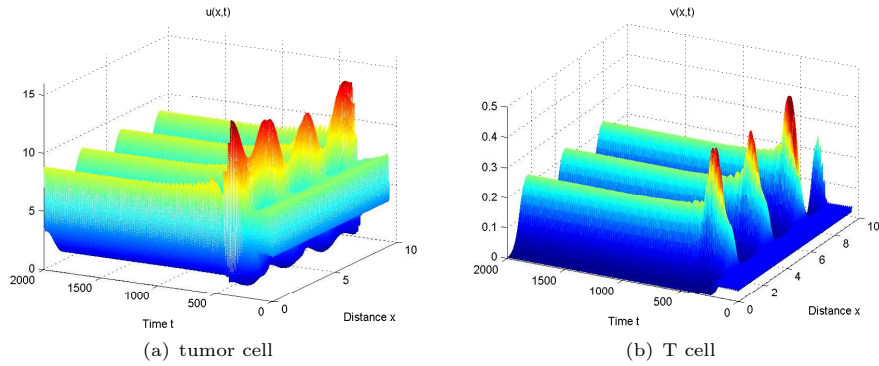


Figure 8. A spatially inhomogeneous periodic solution of (2.2), for $(d_1, \delta) = (0.4473, 0.3455) \in VII$

If we choose the parameter condition (3.1), and $(d_1, \delta) \in I$, then the steady state E_-^* becomes unstable, and there exists a spatially inhomogeneous steady state (induced by Turing bifurcation, which breaks spatial symmetry of system (2.2)) (see Figure 5). If we choose the parameter condition (3.1), and $(d_1, \delta) \in II$, satisfying $\delta < \delta_0$, then the steady state E_-^* is stable (see Figure 1). If we choose the parameter condition (3.1), and $(d_1, \delta) \in III$, then the steady state E_-^* become unstable, there exists a small amplitude homogeneous periodic solution (induced by Hopf bifurcation, which breaks the temporal symmetry of system (2.2)) (see Figure 2). If we choose the parameter condition (3.1), and $(d_1, \delta) \in IV$, the steady state E_-^* become unstable, there exists a large amplitude homogeneous periodic solution (induced by the inactive rate of T cells with the diffusion factors (see Figure 6). If we choose the parameter condition (3.1), and $(d_1, \delta) \in VI$, then the steady state E_-^* is unstable, there exists a large amplitude inhomogeneous periodic solution (induced by the diffusion coefficients and the large inactive rate δ) (see Figure 7). If we choose the parameter condition (3.1), and $(d_1, \delta) \in IIV$, then the steady state E_-^* is unstable, there exists a small amplitude inhomogeneous periodic solution (induced by the diffusion coefficients and the inactive rate δ) (see Figure 8).

By Lemmas 2.3 through 2.5 and Theorem 2.2, we choose the parameter condition (3.1) and the different in-active rate δ of T-cell such as 0.2, 0.3455, 0.3466 and 0.38633 to show the value k of the first Turing bifurcation occurring in Figure 9.

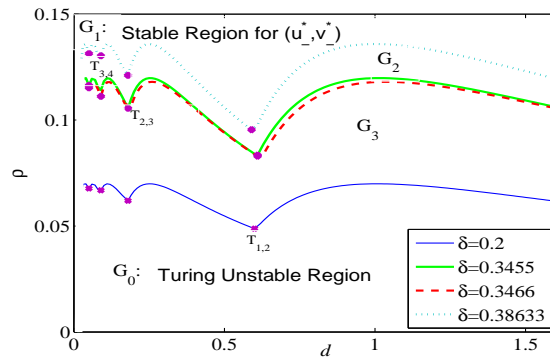


Figure 9. The first Turing bifurcation line $\rho_*(d)$

In Figure 9, the d in $\rho_*(d)$ of (2.19) is the d_1 in system (2.2) and $\rho = d_2/d_1$. Domain G_0 is Turing instable region and domain G_1 is the stable region for E_-^* for four different values of δ . Domain G_2 is the instable region for E_-^* for $\delta = 0.38633$ and is the stable region for the other three different values of δ . Domain G_3 is the stable region for E_-^* for $\delta = 0.2$ and is the instable regions for $\delta = 0.3455$, $\delta = 0.3466$ and $\delta = 0.38633$.

According to Figure 9, if we choose parameter condition (3.1), and $\delta = 0.3455$, $d_1 = 0.75$, $d_2 = 0.056$ (diffusion ratio $\rho = 0.074667 \in G_3$) of system (2.2), then the steady state E_-^* becomes unstable, and there exists an inhomogeneous periodic solution (induced by the small diffusion coefficient and the large in-active rate of T cells) (see Figure 10), in which the small amplitude periodic solution undergoes Turing bifurcation and forms spatially new irregular spatiotemporal patterns(see [21]). The simulation results show that oscillatory Turing or finite wavelength Hopf bifurcation breaks both spatial and temporal symmetry, generating patterns that are oscillatory in space and time [19].

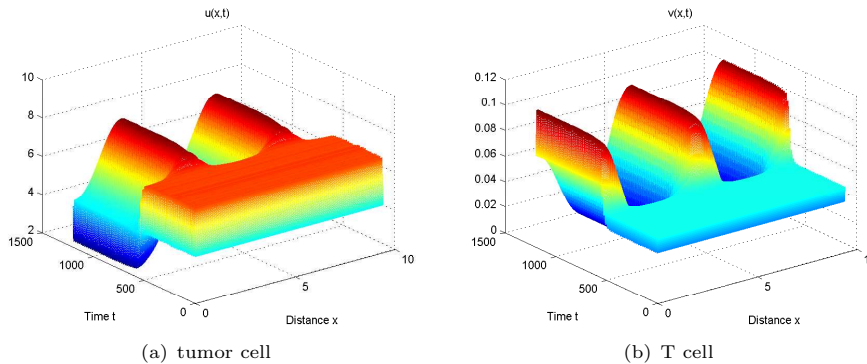


Figure 10. A spatiotemporal solution of (2.2) for the case $\delta = 0.3455$ and $(d_1, d_2) = (0.75, 0.056)$

4. Conclusion

In this paper, we have investigated the spatiotemporal dynamics of combination immunotherapy systems consisting of activated T cells and tumor cells. Our analyses indicate that system (2.2) exhibits complex spatiotemporal patterns via Turing bifurcation and Hopf bifurcation. When parameters are chosen properly, system (2.2) exhibits a spatially homogeneous periodic solution, a spatially inhomogeneous steady state and transient spatially inhomogeneous periodic solutions, which are induced by Hopf bifurcation and Turing bifurcation. In addition, theoretical analysis and numerical results show that the in-active rate of T cells and the diffusion coefficients of T cells and tumor cells are important factors for controlling the spatiotemporal states of T cells and tumor cells. The in-active rate of T cells affects the periodic oscillation of tumor cell number, and the diffusion ratio between tumor cells and T cells affects the space distribution of tumor cell number.

References

- [1] B. Burnet and J. H. Sang, *Physiological genetics of melanotic tumors in drosophila melanogaster. II*, Journal of Genetics, 1964, 49, 233–235.
- [2] X. Cao and W. Jiang, *Turing-Hopf bifurcation and spatiotemporal patterns in a diffusive predator-prey system with Crowley-Martin functional response*, Nonlinear Analysis: Real World Application, 2018, 43, 428–450.
- [3] Y. Jia, *Bifurcation and pattern formation of a tumor-immune model with time-delay and diffusion*, Mathematics and Computers in Simulation, 2020, 178, 92–108.
- [4] W. Jiang, Q. An and J. Shi, *Formulation of the normal forms of Turing-Hopf bifurcation in reaction-diffusion systems with time delay*, Journal of Differential Equations, 2020, 268(10), 6067–6012.
- [5] W. Jiang, H. Wang and X. Cao, *Turing instability and Turing-Hopf bifurcation in diffusive Schnakenberg systems with gene expression time Delay*, Journal of Dynamics and Differential Equations, 2019, 31(4), 2223–2247.
- [6] P. S. Kim, P. P. Lee and D. Levy, *A PDE model for imatinib-Treated Chronic Myelogenous Leukemia*, Bulletin of Mathematical Biology, 2008, 70, 1994–2016.
- [7] D. Kirschner, T. Jackson and J. Arciero, *A Mathematical model of tumor-immune evasion and SIRNA treatment*, Discrete and Continuous Dynamical Systems-Series B, 2012, 4(1), 39–58.
- [8] V. Kuznetsov, I. Makalkin, M. Taylor et al., *Nonlinear dynamics of immunogenic tumors: parameter estimation and global bifurcation analysis*, Bulletin of Mathematical Biology, 1994, 56(2), 295–321.
- [9] M. Nagata, Y. Furuta, Y. Takeuchi et al., *Dynamical behavior of combinational immune boost against tumor*, Japan Journal of Industrial and Applied Mathematics, 2015, 32(3), 759–770.
- [10] N. Nakada and M. Nagata, *Mathematical modeling and analysis of combinational immune boost for tumor elimination*, AIP Conference Proceeding, 2016, 1723, 020002-1–020002-7.
DOI: 10.1063/1.4945058
- [11] B. Niu, Y. Guo and Y. Du, *Hopf bifurcation induced by delay effect in a diffusive tumor-immune system*, International Journal of Bifurcation and Chaos, 2018, 28(11), 145–168.
- [12] K. Paluka and J. Banchereau, *Cancer immunotherapy via dendritic cells*, Nature Reviews Cancer, 2012, 12, 265–277.
- [13] L. Pang, Z. Zhao, S. Liu et al., *Dynamic analysis of an antitumor model and investigation of the therapeutic effects for different treatment regimens*, Computational & Applied Mathematics, 2017, 36, 537–560.
- [14] L. D. Pillis, W. Gu and A. Radunskay, *Mixed immunotherapy and chemotherapy of tumors: modeling, applications and biological interpretations*, Journal of Theoretical Biology, 2006, 238(4), 841–862.
- [15] S. Ruan, *Nonlinear dynamics in tumor-immune system interaction models with delays*, Discrete and Continuous Dynamical Systems-Series B, 2021, 26(1), 541–602.
DOI: 10.3934/dcdsb.2020282

-
- [16] Y. Song, T. Zhang and Y. Peng, *Turing-Hopf bifurcation in the reaction-diffusion equations and its applications*, Communications in Nonlinear Science and Numerical Simulation, 2016, 33, 229–258.
- [17] W. Wang, Q. Liu and Z. Jin, *Spatiotemporal complexity of a ratio-dependent predator-prey system*, Physical Review E, 2007, 75, Article ID 051913.
- [18] X. Xu and J. Wei, *Bifurcation analysis of a spruce budworm model with diffusion and physiological structures*, Journal of Differential Equations, 2017, 262(10), 5206–5230.
- [19] L. Yang, M. Dolnik, A.M. Zhabotinsky et al., *Pattern formation arising from interactions between Turing and wave instabilities*, Journal of Chemical Physics, 2002, 117(15), 7259–7265.
- [20] I. M. Yasinska, I. G. Silva, S. Sakhnevych et al., *Biochemical mechanisms implemented by human acute myeloid leukemia cells to suppress host immune surveillance*, Journal of Cellular Molecular Immunology, 2018, 15(11), 989–991.
- [21] F. Yi, *Turing instability of the periodic solutions for reaction-diffusion systems with cross-diffusion and patch model with cross-diffusion-like coupling*, Journal of Differential Equations, 2021, 218, 379–410.
- [22] F. Yi and A. Eamonn, *The bifurcation analysis of turing pattern formation induced by delay and diffusion in the Schnakenberg system*, Discrete and Continuous Dynamical Systems-Series B, 2017, 22, 647–668.
- [23] J. Zhao and J. Tian, *Spatial model for oncolytic virotherapy with lytic cycle delay*, Bulletin of Mathematical Biology, 2019, 81, 2396–2427.